Pharm Res (2013) 30:1380–1399
DOI 10.1007/s11095-013-0977-8

RESEARCH PAPER

Aggregation and Chemical Modification of Monoclonal Antibodies under Upstream Processing Conditions

Stefan Dengl • Marc Wehmer • Friederike Hesse • Florian Lipsmeier • Oliver Popp • Kurt Lang

Received: 24 June 2012 / Accepted: 4 January 2013 / Published online: 16 January 2013

ABSTRACT

Purpose To investigate antibody stability and formation of modified species under upstream processing conditions.

Methods The stability of 11 purified monoclonal human IgG1 and IgG4 antibodies, including an IgG1-based bispecific CrossMab, was compared in downscale mixing stress models. One of these molecules was further evaluated in realistic bioreactor stress models and in cell culture fermentations. Analytical techniques include size exclusion chromatography (SEC), turbidity measurements, cation exchange chromatography (cIEX), dynamic light scattering (DLS) and differential scanning calorimetry (DSC).

Results Sensitivity in downscale stress models varies among antibodies and results in formation of high molecular weight (HMW) aggregates. Stability is increased in cell culture medium and in bioreactors. Media components stabilizing the proteins were identified. Extensive chemical modifications were detected both in stress models as well as during production of antibodies in cell culture fermentations.

Conclusions Protective compounds must be present in chemically defined fermentation media in order to stabilize antibodies against the formation of HMW aggregates. An increase in chemical modifications is detectable in bioreactor stress models and over the course of cell culture fermentations; this increase is dependent on the expression rate, pH, temperature and fermentation time. Consequently, product heterogeneity increases during upstream processing, and this compromises the product quality.

KEY WORDS aggregation · antibodies · deamidation · fermentation · stress models

ABBREVIATIONS

T_{agg}	aggregation temperature
cIEX	cation exchange chromatography
DSC	differential scanning calorimetry
DSP	downstream processing
DLS	dynamic light scattering
F-Buffer	fermentation-like buffer
HMW	high molecular weight
T_m	melting point temperature
MAb	monoclonal antibody
NTU	nephelometric turbidity units
Re	Reynold's number
SEC	size exclusion chromatography
USP	upstream processing
CHO	chinese Hamster Ovary
IgG	Immunoglobulin G
xMAB	CrossMab
PTFE	polytetrafluoroethylene
PVDF	polyvinylidenefluoride
UV	ultraviolet
PBS	phosphate-buffered saline

INTRODUCTION

Monoclonal antibodies are the most successful and rapidly growing class of biopharmaceuticals (1). As proteins in general tend to be susceptible to various forms of modification

S. Dengl · F. Hesse · K. Lang (✉)
Pharma Research and Early Development, Roche Diagnostics GmbH
Nonnenwald 2
82372 Penzberg, Germany
e-mail: kurt.lang@roche.com

M. Wehmer
Department of Chemistry, Technical University Munich
85748 Garching, Germany

F. Lipsmeier · O. Popp
Pharma Research and Early Development, Roche Diagnostics GmbH
82372 Penzberg, Germany

and degradation, monitoring and controlling antibody stability during production processes constitute one of the major challenges in the development of a successful product. The emergence of novel antibody-based formats (1,2) increases this challenge, as the stability of such molecules may be significantly different from what is known about regular antibody formats.

Large-scale production of monoclonal antibodies involves several steps, including upstream processing (USP, cell culture, fermentation, cell separation), downstream processing (DSP, purification), formulation and storage. In each step, the protein product is exposed to various kinds of stress which can result in unwanted modification of the protein (3,4). Starting in the cell, high expression rates can lead to intracellular aggregation (5) by compromising the correct formation of the native fold and the interaction of nascent chains with molecular chaperones (6). Following secretion into the cell culture medium, the molecules face a multitude of physical stressors, e.g., stirring, turnover of the gas/liquid interface (by sparging the fermentation broth), exposure to various surfaces (7) and elevated temperatures. Chemical stressors such as unfavorable pH (8) and interaction both from components of the fermentation medium and from lysed cells (e.g., proteases) are likewise potentially harmful (3). During purification, product exposure to wide pH, ion concentration, temperature and protein concentration ranges can induce aggregation (9). In addition, the product is exposed to various container and tubing surfaces and to filtration membranes while undergoing physical stress such as that caused by shear forces (10). Finally, great efforts are made to define a formulation that ensures acceptable physical and chemical stability of the drug product for shipping and storage (11). Every modification to the final product carries the risk of diminished biological activity—and thus efficacy—as well as increased immunogenicity (12). The large body of literature available on antibody stability during DSP and on drug product formulation in antibody production reveals relatively little about product behavior in upstream processes. Molecular instability in this first phase of production can either lead to product loss and suboptimal yield, or to modifications that are carried over to subsequent steps and that may be still present in the drug product.

The most prominent degradative pathway in protein production is aggregation, which can occur in all steps of the process (3,4). Various measures are taken to diminish the risk of aggregation, including protein engineering, optimization of process parameters and formulations (13,14). Nevertheless, antibody aggregates can emerge as high molecular weight precipitates, which are removed by filtration, or as soluble forms, which have to be cleared by more elaborate chromatographic methods in DSP.

Chemical modifications to protein molecules are more difficult to detect than aggregation. Product heterogeneity is increased by such modifications, which potentially generate product variants with decreased functionality and/or increased immunogenicity. The risk of promoting various modifications is especially high under USP conditions, due to the highly complex combination of factors that could have an impact on protein stability. One example is the presence of reducing sugars, such as glucose or galactose, which function as carbon sources in the fermentation medium and can lead to non-enzymatic glycation (15). Amino acid oxidation can be favored by sparging the medium and/or by the presence of metal ions and other medium compounds (16). Asparagine deamidation and aspartate isomerization reactions introduce structural and charge heterogeneity into proteins and are promoted at physiological pH and temperature, both of which are conditions found in USP (17,18).

In general, USP conditions stress proteins considerably more than DSP and formulation processes. The reason for this is that USP offers less flexibility for adjusting conditions to protein product requirements and for maximizing stability; conditions instead have to meet the needs of the protein-expressing cells. Thus, while a temperature of approximately 37°C, neutral pH, sparging and stirring are mandatory for mammalian cells to survive in a fermenter, these conditions may be detrimental to the structural integrity of the proteins expressed. In addition, advances in cell culture technology have led to the establishment of routine high-titer processes, achieving product concentrations of more than 10 g/L (19,20). Since aggregation is concentration dependent, these higher titers also increase the risk of aggregation in cell cultures, especially in bioreactors where the protein molecules are exposed to the stressful environment described above. In a study performed by Kiese *et al.*, a monoclonal IgG1 antibody was exposed to stirring and shaking stress models at a concentration of 10 mg/mL (pH6, 25°C). The antibody showed a significant tendency to aggregate under both stress situations (21), which reveals the potential of USP-relevant stress like stirring and shaking to induce protein loss. A further complication is that high molecular weight aggregates are not usually detected in fermentation, because they are removed in subsequent cell separation and filtration steps. As a result, sub-optimal product stability and the resulting product loss usually remain undetected in USP.

To study how different antibodies behave under the physical and chemical stress that can occur in upstream processes, we selected 11 monoclonal human or humanized antibodies produced by CHO cells (9 based on the IgG1 subclass, 2 based on IgG4). The IgG1-based molecules include a new, recently described bispecific format known as "CrossMab" (2). In this molecule, Fab CH1-CL domains are exchanged to achieve correct light chain association in addition to modifications in the Fc-domains ["knobs-into-holes" technology] (22), which direct correct heavy chain pairing. All of these antibodies were selected as lead molecules for the development of a high-titer production and purification process.

We investigated the stability of these antibodies towards different mixing mechanisms under conditions relevant to fermentation. We used stirring- and shaking-stress models similar to ones that were previously described in formulation studies (21,23), that resulted in significant aggregation of antibody molecules. Since stirring and surface turnover (shaking) are relevant stressors in cell culture, we applied these stress models to investigate the effect of cell culture media and media components on the aggregation behavior of antibodies. Product loss due to precipitation and the emergence of soluble aggregates was monitored by SEC. The thermal stability of the molecules under these conditions was determined by DLS and DSC and correlated to stability in downscale stress models. We calculated physical properties of the downscale mixing stress test and compared them to the properties of a real bioreactor. Since physical stress in the downscale mixing stress tests did not fully represent stress in a bioreactor, one of the tested antibodies was stressed under realistic fermentation conditions in bioreactors and was used for an in-depth analysis of the resulting aggregation, chemical modification and influence of medium components and fermentation parameters on these degradation pathways. Finally, we analyzed the modifications that occur in real cell-culture fermentations together with the kinetics of the observed modifications. In general, we focus on the molecules that remain in solution when challenged with fermentation-relevant stress, and are thus part of the final product.

The results presented here have an impact on the design of chemically defined fermentation media and of fermentation process parameters, in order to maximize stability and homogeneity of the protein product.

MATERIALS AND METHODS

Materials

Buffers and Media

Stress tests were carried out in two basic formulations: first, a fermentation-like buffer (F-buffer) containing 10 mM Hepes/NaHCO3, 4 g/L glucose, 100 mM NaCl, 5 mM KCl, pH 7.0, and second, a chemically defined CD CHO fermentation medium (Gibco), which was prepared according to the manufacturer's instructions. Cell culture fermentations were carried out with an in-house medium platform.

Excipients such as Brij 35, Myristyl-sulfobetaine SB3-14, β-cyclodextrin, Poloxamer 188 (Sigma-Aldrich), n-D-β-Maltopyranoside, FOS-Choline 12 (Anatrace®, Affymetrix), Triton X-100, CHAPS (Roche), Tween 80, PEG 300, PEG 4000, PEG 20000, Methy-β cyclodextrin (Fluka), Tween 20, trehalose and arginine (Merck Millipore) were solubilized in buffer (when necessary) and sterile filtered using 0.22 µm Millex® GV (PVDF) syringe filter units (Millipore). The sterile filters were saturated with surfactant solution before filtration to minimize adsorption to the filtration membranes.

Antibodies

Eleven different recombinant monoclonal, fully human or humanized antibodies were obtained from fed-batch fermentations of stably transfected CHO cells. The purified antibodies were obtained in different formulations and were all at least purified by Protein A chromatography. Soluble aggregates were removed by SEC when the soluble monomer content was <95%. Overall purification yield was ~60–80% with regard to the antibody amount detected in cell culture harvests by analytical Protein A chromatography. The concentration of the purified antibodies was determined by UV absorbance at 280 nm using the molar extinction coefficient calculated for each molecule (24). The calculated isoelectric points (p*I*) were all in the range of pH 8.4–9.3.

Downscale Stress Tests

Stirring Stress

Antibodies were formulated by dialysis into the respective buffer or medium using Slide-A-Lyzer® cassettes (10 K MWCO, Thermo Scientific). Dialysis was carried out in two steps for 3–5 h and overnight. All samples were sterile filtered using 0.22 µm Millex® GV (PVDF) syringe filter units (Millipore). Five milliliters of sterile antibody solutions were filled in 10 mL brown serum bottles containing 15 mm x 4.5 mm PTFE coated stirrer bars (Carl Roth GmbH). Serum bottles were closed with metal screw caps with a PTFE septum (Carl Roth GmbH). The antibody concentration was adjusted to 4–5 mg/mL and solutions were stirred continuously at 300 rpm and 37°C. In this setup, no extensive vortex was formed and no splashing of liquid was observed. Thus, stress induced instabilities of antibodies are mainly resulting from stirring and not from turnover of the air/liquid-interface. To test the influence of the stirring method on MAb stability, a small scale, top-stirring system was constructed, whereby the stirrer bar was attached to a rotatable needle, which, in turn, was fixed to the serum bottle by two screw caps. This arrangement allowed the stirrer to move at 300 rpm without touching the glass surface at the bottom.

For both downscale stirring models, physical parameters were calculated: the ratio of impeller diameter/tank diameter (D/T) is 0.75. The impeller tip speed was calculated with the formula $v=N \cdot D \cdot \pi$, where N is the rotation speed and D is the impeller diameter. For both downscale stirring models the impeller tip speed is 0.2355 m/s. The Reynold's number (Re) was calculated with the formula $Re=(\rho \cdot N \cdot D^2)/\eta$, where ρ is the density and η is the dynamic viscosity. For our calculations we used values of 993 $kg \cdot m^{-3}$ for ρ and 0.0007 $m^{-1} \cdot s^{-1}$ for η, which are typical values for

aqueous solutions at 37°C. The resulting Re is 1595.9 at 300 rpm for both downscale stirring systems, indicating non-turbulent fluid dynamics. The resulting bulk velocity [(Re · η)/(ρ · D)] is 0.075 m/s for both downscale stirring models.

Two hundred microliter were withdrawn from the downscale reactors at different time points using 1 mL syringes. Samples were immediately filtered through 0.22 µm Acrodisc® LC13 mm syringe filters (Pall Corporation) and used for analyzing the soluble antibody species by analytical SEC.

Shaking Stress

Antibody solutions were prepared as described for downscale stirring stress. The setup used was the same as that described for stirring stress only without the stirrer bar. The serum bottles were shaken horizontally and radially at 200 or 300 rpm (KS 260 basic, IKA®) and 37°C. Two hundred microliter were removed under sterile conditions at different time points. The samples were filtered and analyzed by SEC as described for the downscale stirring stress samples.

Modification Under Conditions Relevant to Fermentation

Antibody solutions were prepared by diluting a 52.4 mg/mL MAb solution in 35 mM acetate, pH5.0, to 5 mg/mL under test conditions. All solutions were sterilized by filtration using 0.22 µm Millex® GV (PVDF) syringe filter units (Millipore) before use. Five hundred microliter of each sample were filled into sterile plastic tubes and incubated without agitation at 37°C. Fifty microliter were removed at different time points for cation exchange chromatography.

Bioreactor Stress Tests

Sterilized Sartorius Biostat® B-DCU3 Quad 2 L systems were filled with 1.5 L of antibody solution. MAb4.2 in 35 mM acetate pH5.0 was concentrated to 52.4 mg/mL using Sartocon Slice Cassettes (Hydrosart®, 0.1 qm, MWCO 30 kDa) in a Sartocon Slice SF alpha setup. The concentrated MAb-solution was diluted to a concentration of 5 mg/mL in the corresponding buffer or medium and filtered with Sartopore®2 150 0.2 µm+0.1 µm filters (Sartorius-Stedim).

The bioreactors were operated using a Biostat® B-DCU (Sartorius). Stirring speed and temperature were kept constant at 350 rpm and 36.5°C, respectively. The pO2 was recorded using an InPro® 6800 sensor, and the pH was measured using an InPro 3253 electrode (both Mettler Toledo). The pH was automatically regulated at a setpoint value of pH7.0 with a deadband of ±0.3 by addition of either CO_2 or NaOH. No regulation was necessary, however, as all pH values were found within the deadband over the course of the entire experiment. Bioreactors were sparged with sterile air at 20 ccm/min when aeration was used as an additional stressor. After 200 h, 75 mL of sterile 1% (v/v) antifoam suspension (Medical antifoam C emulsion, Dow Corning®) was added for a final concentration of 0.05% (v/v).

Initial samples were taken after 4 h, then twice daily at intervals of 16 h and 8 h (deviations from this routine can be seen in Fig. 2). Five milliliters were drawn by syringe from each bioreactor and immediately analyzed with a pHOx blood gas analyzer (Nova Biomedical) to obtain pH, pO_2 and pCO_2 values. The solutions were immediately filtered for SEC using 0.22 µm Acrodisc® LC13 mm syringe filters (Pall Corporation). Selected samples were used for turbidity measurements prior to filtration (see below).

The Reynold's number for the bioreactor stress test in F-buffer was calculated as described for the downscale stress models. The Re = 19930.5 at 300 rpm and 23252.2 at 350 rpm. Both values indicate turbulent fluid dynamics.

Cell Culture Fermentation

Fermentations were performed in fully controlled Sartorius Biostat® B-DCU3 Quad 2 L systems. Physical parameters (pH, temperature, and pO2) were monitored online. pH was controlled by a carbonate buffer system within the medium, CO_2 gassing, and 1 M $NaHCO_3$ solution. pO_2 was controlled by aeration rate, stirrer speed, and oxygen gassing. A proprietary medium and feed were used for cell culture fermentation. Cells producing a humanized monoclonal antibody were inoculated with 3×10^5 viable cells/mL and cultured for 13 days.

Analytical Methods

Size Exclusion High Performance Liquid Chromatography (SEC)

Two hundred microliter of the downscale stress samples were applied to a TSK-GEL® QC-PAK GFC 30 7.8 mm × 15 cm gel filtration column (Tosoh Biosciences) at a flow rate of 1 mL/min. Fifty microliter of the bioreactor stress samples were applied to a Superdex™ 200 HR 10/30 column (GE Healthcare) at a flow rate of 0.75 mL/min. 2x PBS pH7.4 was used in both cases as the mobile phase on an UltiMate® 3000 HPLC system (Thermo Scientific). Elution of protein from the column was recorded at 280 nm and 220 nm. Monomer peaks were integrated using the Chromeleon® software (version 6.8, Thermo Scientific) and monomer content of the samples was expressed as monomer peak area (mAU x min).

Dynamic Light Scattering (DLS) and Differential Scanning Calorimetry (DSC)

Aggregation temperatures of antibodies were analyzed by detecting the onset temperature of large particle formation

by dynamic light scattering. Samples of the antibodies in buffer or in medium were prepared for this analysis at a concentration of 1 mg/mL. For DLS, 37 µL of each sample were filtered by centrifugation at 1,000 g for 1 min. into an optical plate (Corning® 348 well clear bottom microplate), using a filter plate (Multiscreen® HTS 384-well HV, 0.45 µm PVDF membrane, Millipore) to remove potential particles. Twenty microliter of paraffin oil was immediately added to each well to prevent sample evaporation. A DynaPro™ Plate Reader (Wyatt) with an 830 nm laser was used for DLS measurements. The plate was continuously heated from 25°C to 80°C at a rate of 0.05°C/min. Data were evaluated with the Dynamics® software (version 7.0.2.7, Wyatt Technology Corp.). T_{agg} was defined as the temperature at which the average particle size R rises 1 nm above the baseline.

Differential scanning calorimetry (DSC) measurements were performed using a N-DSC II microcalorimeter (Calorimetry Sciences Corporation). Protein melting point values (T_m) were obtained from peaks in the temperature dependent specific heat capacity graphs.

Turbidity

Samples were transferred to particle-free glass cuvettes (Hach Lange) and the turbidity measurements were performed using a HACH 2100 IS turbidimeter (Hach Lange) calibrated against formazine suspension standards. Results are expressed as nephelometric turbidity units (NTU).

Cation Exchange High Performance Liquid Chromatography (cIEX)

Seventy five microgram of each sample were applied to a ProPac™ WCX-10 4×250 mm column (Thermo Scientific) equilibrated with 20 mM MES, 5 mM NaCl (pH6.5, flow rate of 1 mL/min.). Bound antibodies were eluted with a linear salt gradient of 5 to 200 mM NaCl over 35 min. Samples from cell culture fermentations were dialyzed into 20 mM histidine, 140 mM NaCl, pH6.0 using Slide-A-Lyzer® cassettes (10 K MWCO, Thermo Scientific) before application to the cation exchange column. Elution of antibody charge variants was monitored at 280 nm. Chromatograms were evaluated with the Chromeleon Software (version 6.8, Thermo Scientific). This was carried out by integrating the total peak area of all eluting species and calculating the relative percentage of the main peak area. The fraction of the main peak (% main peak) was then used as a relative measure of the extent of modification.

Quantitative Protein A Chromatography

Fermentation samples were filtered and applied to a Poros® Protein A 2.1×30 mm column (Applied Biosciences) with 2x PBS, pH7.4, for 1 min at a flow rate of 2.5 mL/min. Bound antibodies were eluted with 550 mM acetic acid for 1 min at 2.5 mL/min. The area of the resulting peak was used for calculating the amount of the bound antibody. A calibration curve of the same antibody in the range between 7.7 and 120 µg was prepared for this purpose.

Cell Densities and Viability

Viable and total cell densities were evaluated along with viability using the trypan blue exclusion staining method. An automated Cedex HiRes system (Roche Diagnostics) was used for analyzing more than 10 pictures per sample and day according to the manufacturer's specifications.

$$\text{Cell viability} = N_{\text{Trypan blue}-} / \left(N_{\text{Trypan blue}-} + N_{\text{Trypan blue}+} \right) * 100\%$$

Calculation of Modification Rates and Half-Lives

For all stress test samples, the percentage of the cIEX main peak area at the start of the corresponding experiments was normalized to 100%. Values for relative peak areas in stressed samples were calculated as fractions of the peak area at t0. The resulting data were fitted to a first-order exponential decay curve with the program XLfit™ (IDBS):

$$N(t) = N_0 \, e^{-kt}$$

where t is time, N is % main peak at time t, N0 = 100 and k is the decay constant.

Half-life values for the main peaks were calculated by:

$$t_{1/2} = \ln 2 / k$$

No t0 was available for samples from cell culture fermentations. In this case, the extent of modification was expressed as the relative percentage of the main peak in relation to the cIEX total peak area for each sample. The R statistical software (http://www.R-project.org/) with the additional pspline package (http://CRAN.R-project.org/package=pspline) was used for spline fitting and subsequent calculations.

RESULTS

Aggregation of Antibodies under Upstream Processing Conditions

Aggregation of Antibodies in Downscale Stress Tests

In the process of fermentation, antibodies are secreted from cells into a fermentation medium that is agitated by stirring both to ensure mixing of cells and medium components and

to properly disperse oxygen that enters the fermenter through the sparger. Continuous aeration of bioreactors adds another type of stress in the form of extensive air-liquid interface turnover, which is commonly known as a site of protein aggregation (23,25,26). We analyzed the aggregation behavior of 11 antibodies (9 IgG1-based antibodies with 1 CrossMAbXMAb format and 2 IgG4-based antibodies) in response to these predominant fermentation-related stresses in downscale models.

For these stress experiments we used two basic formulations:

1. A buffer containing only basic elements of chemically defined fermentation media, such as sugar, salts and a pH buffered at 7.0 (F-buffer, see Materials and Methods). Because excipients that are known to efficiently protect against aggregation (apart from sugar) are lacking in this formulation, these conditions represent an "unprotected" environment demonstrating the intrinsic instability of the molecules towards the relevant stress.
2. A commercial fermentation medium that is broadly used for producing therapeutic proteins from Chinese hamster ovary cells. These conditions represent the realistic environment of the chemically defined medium in which antibody molecules are incubated during fermentation.

Downscale Stirring Stress. The setup used was similar to stirring stress models published in the literature, where antibody formulations are stirred in closed glass vials at a constant speed and temperature (21). These downscale models are usually used in formulation studies and are not designed to exactly reproduce physical stress in real bioreactors. However, they can be readily used to easily compare antibody behavior towards fermentation-relevant mixing mechanisms like stirring and surface turnover (shaking). We used 300 rpm of stirring speed, which is a typical average stirring speed of fermentations in bioreactors. Additionally, 300 rpm were optimal for simultaneous analysis of fast and slow aggregating antibodies in the chosen timeframe. After 0, 24, 48, 72 and 144 h of stress, aliquots were removed from the vials and analyzed for the content of remaining intact antibody monomer. The solution was filtered for this study to remove precipitate/HMW aggregates. This corresponds to a post-fermentation filtration step that removes particles from the fermentation supernatant before it is used for purification in downstream processing. Stirring in F-buffer resulted in visible precipitation for most of the antibodies after only 24 h of stress. We detected a linear decrease of the SEC monomer peak area over time, as exemplified in Fig. 1a for xMAb1.1, MAb1.2 and MAb4.2. The same decrease was detected for the total protein, measured by UV-absorption, before the samples were applied to the SEC column (data not shown). We did not detect soluble aggregated species by SEC for any one of the 11 antibodies (shown for MAb 4.2 in Fig. 1b), thus the loss of antibody monomers induced by stirring is explained by the formation of precipitates that are removed by the filtration step. The linear decrease of monomer peak area was converted into an aggregation rate that is expressed as the percentage of antibody monomer lost per hour (%MAb/h, Table I). Figure 1c depicts the aggregation rates for all antibodies in F-buffer and in the fermentation medium. The instability of MAbs towards stirring stress is much higher in F-buffer (dark bars). Strikingly, the inherent instability of the 11 antibodies varies widely, with MAb1.3 and MAb1.7 (0.12% MAb/h each) being the most stable, and MAb1.6 (0.56% MAb/h) and the two IgG4-based MAbs (0.5% and 0.7% MAb/h for MAb4.1 and MAb4.2, respectively) showing the highest instability. This means a ~6-fold higher instability for MAb4.2 compared to the antibodies with the highest stability under the chosen conditions. This corresponds to a 2.9–17% loss of antibody monomer per day for the molecules tested. Interestingly, the stability of the new CrossMab format (intermediate stability = 0.4% MAb/h) is comparable to other IgG1 antibodies without domain exchange.

When stirred in medium, aggregation for the majority of the tested antibodies was 75–100% less than that observed with F-buffer (Table II). The aggregation rate here is at least 58% less (MAb1.8) than that observed with F-buffer, up to complete inhibition of aggregation (xMAb1.1 and Mab1.2).

Aggregation was caused exclusively by the stirring stress. Antibodies were stable both in F-buffer and in the fermentation medium when incubated under identical conditions but without stirring (data not shown).

The choice of stirring method is an important factor in stress tests and has a huge impact on the resulting observed stabilities (27). For this reason we investigated an additional stirring method in our downscale model. We constructed small stirrer devices that were suitable for the vials described above except that, in this case, the stirrer bar entered the antibody solution from the top without contacting the glass surface of the serum bottle (see sketch in Fig. 1c, on the right). Dimensions and physical parameters like the impeller diameter/tank diameter ratio (D/T), impeller tip speed and Reynold's number were identical for both downscale models (see Materials and Methods section). We tested the stabilities of MAb1.2 and MAb4.2 in F-buffer in these devices. The aggregation rates were significantly lower for both

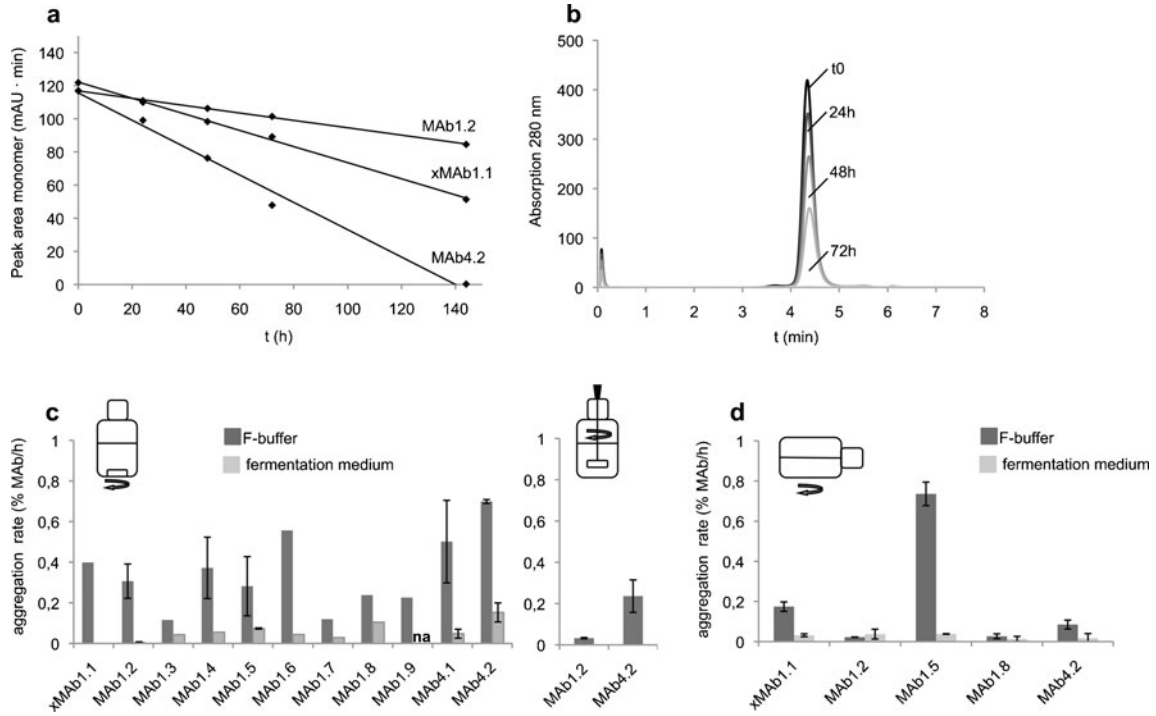

Fig. 1 Aggregation of 11 antibodies in downscale fermentation stress tests. **a** Monomer loss over time of 3 different antibodies (IgG1, IgG1 CrossMab and IgG4) in F-buffer stressed by stirring in the downscale stress experiment. Shown is the reduction of SEC monomer peak area (mAU*min) over time as exemplified in (**b**) for MAb4.2. **c** Aggregation rates of antibodies stressed by stirring in 2 different solvent systems. Left graph, stirring stress of 11 antibodies in "bottom-stirrer" devices. *Error bars* are indicated when multiple experiments were carried out: 5 (F-buffer) and 5 (fermentation medium) experiments for MAb1.2; 2 and 1 experiments for MAb1.4; 2 and 2 experiments for MAb1.5; 2 and 2 experiments for MAb4.1; 4 and 5 experiments for MAb4.2. Right graph, stirring stress of 2 antibodies in "top-stirrer devices" in F-buffer. Error bars result from 2 experiments for MAb1.2 and 4 experiments for MAb4.2. **d** Aggregation rates of 5 different antibodies stressed by shaking in 2 different solvent systems. *Error bars* are indicated when multiple experiments were carried out: 2 (F-buffer) and 3 (fermentation medium) experiments for xMAb1.1; 3 and 2 experiments for MAb1.2; 2 and 2 experiments for MAb1.5; 3 and 3 experiments for MAb1.8; 3 and 2 experiments for MAb4.2. *na* not available.

antibodies in the "top-stirrer" systems. The aggregation rate for MAb1.2 was 90% lower than the rate in F-buffer in the "bottom-stirrer" stress test; the MAb4.2 rate decreased by 66%.

Table I Aggregation Rates (%MAb/h) of Monoclonal Antibodies in Downscale Stress Experiments. (see Figs. 1c, d and 3a. Shown are the Mean Values Rounded to Two Decimal Places)

	Stirring				Shaking	
Antibody[a]	F-buffer	Medium	"top-stirrer" F-buffer	F-buffer+0.01% Tween 20	F-buffer	Medium
xMAb1.1	0.40	0	–	0	0.17	0.03
MAb1.2	0.31	0	0.03	0.02	0.02	0.04
MAb1.3	0.12	0.04	–	0.02	–	–
MAb1.4	0.37	0.06	–	0.12	–	–
MAb1.5	0.28	0.07	–	0.07	0.74	0.04
MAb1.6	0.56	0.04	–	0.24	–	–
MAb1.7	0.12	0.03	–	0.01	–	–
MAb1.8	0.24	0.10	–	0.14	0.03	0.01
MAb1.9	0.23	–	–	0.13	–	–
MAb4.1	0.50	0.05	–	0.12	–	–
MAb4.2	0.70	0.15	0.24	0.74	0.09	0.02

xMAb1.1 = IgG1-based bispecific cross-MAb (2)

[a] The first number indicates the antibody subclass: 1 for IgG1 and 4 for IgG4

Table II Humanized Monoclonal Antibodies in Downscale Stress Experiments

Antibody	T_{agg} in F-buffer/fermentation medium [°C] DLS	Reduction of aggregation rate in medium (stirring stress, see Fig. 1c)[b]	Reduction of aggregation rate in F-buffer+0.01% Tween 20 (stirring stress, see Fig. 3a)[b]	Δ soluble aggregates shaking stress in F-buffer[c]	Δ soluble aggregates shaking stress in medium[c]
xMAb1.1	61.8/58.8	100%	100%	8,8%	0,4%
MAb1.2	68.7/66.7	100%	94%	0,1%	0,3%
MAb1.3	70.2/70.6	66%	83%	–	–
MAb1.4	62.6/58.2	84%	68%	–	–
MAb1.5	51.2/49.4	75%	75%	0%	0.5%
MAb1.6	60.8/59.4	93%	57%	–	–
MAb1.7	61.5/59.8	75%	92%	–	–
MAb1.8	65.5/n.a.[a]	58%	42%	1,3%	0,3%
MAb1.9	65.8/64.1	n.a.[a]	43%	–	–
MAb4.1	58.8/59.6	90%	76%	–	–
MAb4.2	60/58.7	79%	0%	1,9%	1,6%

[a] Not available

[b] Shown is the reduction in the aggregation rate [%MAb/h] of antibodies under the conditions indicated compared to F-buffer in the downscale stirring stress test

[c] Increase in the SEC peak area of soluble dimers and oligomers over the course of 72 h of shaking stress

In summary, antibody response to stirring stress varied greatly in our setup. Aggregation rates are high in an "unprotected" environment (F-buffer), but the use of a fermentation medium significantly increases the stability of all antibodies.

Downscale Shaking Stress. To simulate the stress of gas/liquid interface turnover in a downscale model system, the glass vessels we used were the same as those in the downscale stirring stress experiments. This was done to exclude unspecific aggregation effects that could be induced by exposing the molecules to different solid surfaces. The glass vessels were fixed horizontally on a radial-horizontal shaker at 37°C. In initial experiments we evaluated different shaking speeds to find a stress condition which allowed us to evaluate fast and slow aggregating antibodies simultaneously in a timeframe similar to that used for studying downscale stirring stress (data not shown). Two hundred revolutions per minute was chosen based on these results. Five different antibodies were used in these stress experiments: xMAb1.1, MAb1.2, MAb1.5, MAb1.8 and MAb4.2. Small aliquots of the stressed samples were removed after 0, 24, 48 and 72 h, filtered, and the monomer content was analyzed by SEC. As in the stirring-stress experiments, we observed varying susceptibility towards shaking stress for the different MAbs in F-buffer (Fig. 1d). The aggregation rate was highest in MAb1.5 (0.74% MAb/h), followed by xMAb1.1 (0.17% MAb/h). MAb1.2, MAb1.8 and MAb4.2 showed a relatively low tendency to aggregate (<0.1% MAb/h). The rates observed for aggregation induced by shaking stress did not fully correlate to the rates for stirring stress. Four of the 5 antibodies showed a significantly lower aggregation rate for shaking stress than for stirring stress. MAb1.5 is the exception with a 2.6-fold higher susceptibility towards shaking stress in F-buffer (Table I).

In comparison to downscale stirring stress, we detected the emergence of soluble aggregates in the SEC chromatograms for some of the tested antibodies (Table II). The highest value was detected for xMAb1.1, for which soluble dimers and oligomers increased by 8.8% after 72 h of shaking stress in F-buffer. Whereas negligible amounts were detected for MAb1.2 and MAb1.5, MAb1.8 and MAb4.2 showed small increases of 1.3% and 1.9%, respectively. Medium components seem to prevent the formation of soluble aggregated species. Inhibition was nearly complete for xMAb1.1, and MAb1.2. MAb1.5 and MAb1.8 likewise showed negligible amounts of soluble aggregates after 72 h of shaking in medium. Interestingly, formation of MAb4.2 dimers and oligomers was not reduced as significantly as was the case with the other antibodies when shaken in medium. After 72 h, an increase of 1.6% was still detectable. In contrast to the results of our downscale stirring stress studies, we found the reproducibility of some of the antibodies shaken in F-buffer to be poor. Strikingly, this was only seen among different experiments carried out at different times, and not within one set of experiments carried out on 1 day (data not shown). We could not attribute this to the quality of antibody samples, because identical batches were used. The reason for the poor reproducibility may therefore be that the affected MAbs are highly sensitive to the slightly different conditions that arise when experiments are carried out at different times by different experimenters. However,

aggregation rates for all the tested samples were highly reproducible when the MAbs were shaken in fermentation medium. All MAbs showed negligible aggregation (<0.05% MAb/h, Fig. 1d), which is comparable to the findings for stirring stress in a medium. We exclude p*I*-dependent effects for the observed differences in aggregation, since all antibodies show calculated p*I*s in the range of pH8.4–9.3 which is well above the pH of the F-buffer and the fermentation medium.

Thermal Stability of Antibodies Under Conditions Relevant to Fermentation

A common measure for the intrinsic stability of proteins is the aggregation temperature T_{agg}. When a protein is heated above its characteristic thermal stability point in a given formulation, unfolding exposes hydrophobic parts that are buried in the native fold. At this point, the protein molecules start to aggregate, which can be measured by various techniques. We used dynamic light scattering to analyze the aggregation point of the 11 antibodies in F-buffer and in a fermentation medium in order to compare the resulting T_{agg} to the stability results from the downscale stress tests. The T_{agg} values are summarized in Table II. In general, the onset of aggregation in F-buffer was above 60°C for the majority of the antibodies (exceptions were MAb1.5 and MAb4.1). The T_{agg} values for antibodies in fermentation medium were slightly lower compared to F-buffer in the range of 1.3–4.4°C. Only Mab1.3 and Mab4.1 showed slightly higher T_{agg} values in medium (+0.4°C and +0.8°C, respectively). We did not find a general correlation of aggregation temperatures with aggregation rates in downscale stirring and shaking stress.

In addition, we performed differential scanning calorimetry (DSC) for three antibodies. Melting temperatures (T_m) for xMAb1.1, MAb1.2 and MAb4.2 in F-buffer and fermentation medium were determined from temperature dependent specific heat capacity graphs. The obtained transition temperatures were 72.6°C and 79.5°C for xMab1.1 and 71.5°C and 82.2°C for Mab1.2. For Mab4.2 we measured transitions at 68.2°C and 76.2°C. In general, T_m values obtained in medium were slightly lower than in F-buffer (data not shown) which corresponds to the results obtained by DLS. MAb4.2 shows lower melting temperatures compared to Mab1.2 and xMAb1.1 as frequently observed for IgG4 and IgG1 (28). xMAb1.1 and Mab1.2 show T_m values that are in the range usually observed for IgG1 antibodies (29). The transition temperatures obtained for xMAb1.1 are a few degrees higher as in the original publication of this molecule (2), which we account on the different formulations used for the measurements.

The stability of the 3 antibodies determined by DSC correlates with the sequence of the aggregation temperatures observed by DLS (Table II). The differences in thermal stability reflect the relative sensitivity towards stirring stress with Mab1.2 being the most stable and Mab4.2 the least stable antibody (Table I). In contrast, sensitivity towards shaking stress shows no correlation to thermal stability. Mab1.2 again is most stable during shaking but here Mab4.2 is more stable than xMab1.1. Please note that T_{agg} is in general lower than T_m because it represents the onset of a change in particle size, whereas T_m represents the transition temperature where ~50% of the protein structure is unfolded. Unexpectedly, the T_{agg} of xMAb1.1 (Table II) was slightly lower than expected from the DSC-thermogram, whereas there is a good correlation between the DLS and DSC data of Mab1.2 and Mab4.2.

In summary, we observed no general correlation between the T_{agg} or T_m and the aggregation rates in the downscale stress tests, indicating that the behavior of antibody molecules under mechanical stress such as stirring and shaking cannot be fully predicted from their thermal stability alone.

Aggregation of Antibodies in Bioreactors

In the experiments described so far we investigated several stress conditions that are related to upstream processing, such as stirring stress and gas/liquid interface turnover (shaking stress) in downscale models. The results show highly variable stabilites of antibody molecules towards different mixing mechanisms that are also relevant to cell culture fermentations. However, the downscale mixing models are not representative for the physical stress in a real bioreactor. This is made clear by comparing the difference in the Reynold's numbers of the downscale stirring stress models (1595.9 at 300 rpm) and a 2 L bioreactor (19930.5 at 300 rpm, see Materials and Methods). Therefore, the observed instabilities in the downscale mixing models may not be representative for real bioreactor cell cultures. To obtain a more realistic view of the response of monoclonal antibodies towards stress under realistic fermentation conditions, we performed large-scale stress tests in 2 L bioreactors at a concentration of 5 mg/mL as achieved during cell culture production of monoclonal antibodies (19,20,30). The IgG4-based MAb4.2 was chosen for these experiments because it showed the highest aggregation rates in F-buffer as well as in fermentation medium (Table I and Fig. 1c). In addition, the formation of soluble MAb4.2 aggregates was not significantly diminished by components of the fermentation medium (Table II). Two conditions were chosen to allow a direct comparison to the results obtained in the downscale experiments: F-buffer and fermentation medium. Furthermore, the antibody was stressed by sparging with sterile air at 20 ccm/min in fermentation medium in a separate bioreactor. This condition is expected to realistically simulate the physical stress of a real fermentation.

The resulting aggregation in bioreactors was significantly lower than in the downscale stress tests. In F-buffer, the SEC monomer peak area was only found to decrease by <1% (Fig. 2, left graph); in the medium, however, we measured a more significant decrease in SEC monomer peak area for both the sparged (−5.5%) and the unsparged (−4.3%) bioreactor within 360 h (Fig. 2, right graph). A simultaneous increase in soluble SEC aggregate species was detected in medium (Fig. 2, lower graphs). A linear increase of ~1% was detected during the experimental time when F-buffer was used. The detected soluble species were exclusively antibody dimers as judged by SEC retention time. Accordingly, the increase in soluble species in the fermentation medium was 4.3% for the unsparged and 5.5% for the sparged medium, whereby the detected species were mainly antibody dimers and, in some cases, higher molecular weight aggregates. The total protein content in each bioreactor (measured by UV absorption at 280 nm) was constant throughout the experiment.

We evaluated additional parameters relevant to fermentation that could compromise the stability of this antibody. We began by adding an antifoam suspension to a final concentration of 0.05% (v/v) after 200 h (light gray phases in Fig. 2). The SEC monomer peak area did not indicate that any product loss was induced by the addition of this substance to either the F-buffer or the medium. The slight increase in turbidity can be explained by the turbid nature of the antifoam suspension itself. After 315 h we introduced a 20 ccm/min sterile airflow to MAb4.2 in F-buffer (dark grey phase in Fig. 2, left graph). This was followed by an increase in turbidity at a rate ~20 fold faster than was found in the phase without sparging or antifoam, indicating that MAb4.2 aggregation increases in sparged F-buffer. However, this increase in turbidity did not result in a measurable decrease of antibody SEC monomer peak area which suggests that aggregation is only marginal and detectable by turbidity measurements alone. By contrast, no increase in turbidity was detected in the fermentation medium, which was true for both the unsparged and the sparged bioreactor.

In summary, MAb4.2 stability was only marginally affected in bioreactors. This was unexpected in light of the results from downscale experiments in which antibodies showed extensive aggregation when stirred in the same F-buffer and fermentation medium. In this case, HMW aggregate formation in F-buffer was only detectable by an increase in turbidity that did not manifest in a detectable product loss. The addition of antifoam had no significant effect, but sparging the buffer with sterile air increased the turbidity of the solution. This effect was not detected in the sparged medium, in which the antibody was fully protected from any signs of aggregation, except for an increase of soluble aggregate species.

Stabilization of Antibodies Against Aggregation in Upstream-related Stress

Under both downscale and bioreactor stress, the tested antibodies showed detectable formation of HMW aggregates in F-buffer. On the other hand, HMW aggregates were was either diminished dramatically (downscale stress) or completely inhibited (bioreactor) when the molecules were stressed in the chemical environment of a fermentation medium.

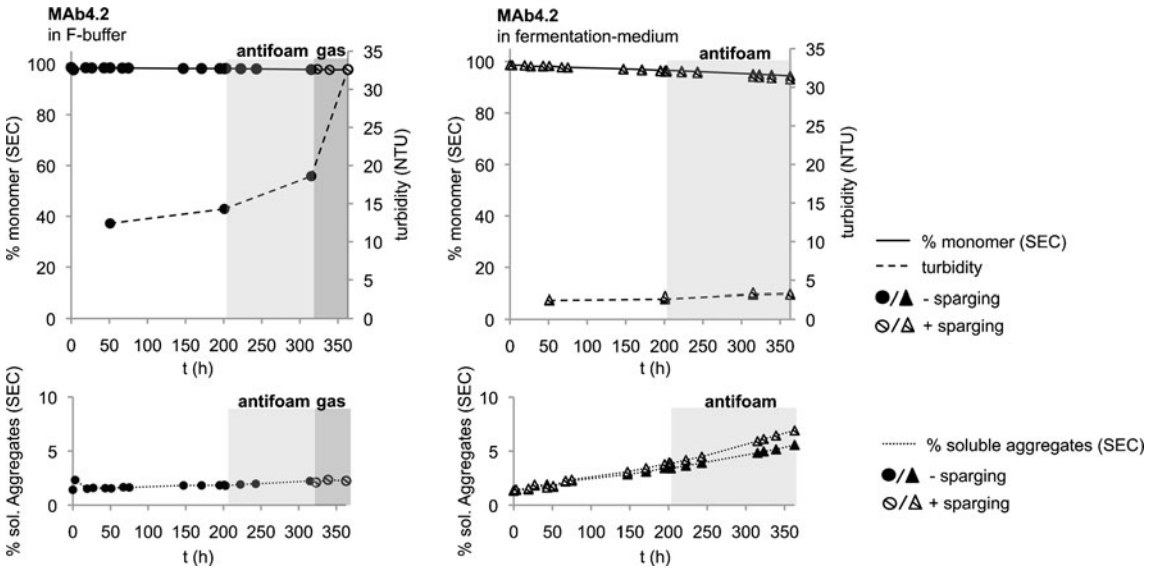

Fig. 2 Fermentation-relevant stress of MAb4.2 in bioreactors. Stirring stress studies of MAb4.2 in 2 L bioreactors in F-buffer (*left*) and fermentation-medium +/- sparging (*right*). The lower graphs show the relative amounts of soluble aggregates. "% Monomer (SEC)"and "% sol. aggregates (SEC)" are calculated as the respective relative peak areas of each chromatogram. Two experimental phases are indicated in *light gray* (addition of 0.05% (v/v) antifoam) and in *dark gray* (addition of 20 ccm/min sterile airflow, only F-buffer).

We conducted tests to determine whether stabilization similar to that observed in fermentation medium can be obtained in a modified F-buffer. Tween 20 (Polysorbate 20) was chosen as a potential stabilizing substance because Tween 20 and other surfactants are well known as potent inhibitors of agitation-induced protein aggregation (21,31,32). It was also shown that addition of Tween 20 dramatically reduces aggregation of human G-CSF when added to the culture medium (33). To evaluate the impact of this surfactant on the stability of the 11 antibodies in the downscale stirring model, we modified the F-buffer with 0.01% (w/v) Tween 20.

Ten of the 11 antibodies showed significantly reduced aggregation rates upon the addition of Tween 20 (Table I and Fig. 3a). The aggregation rate is reduced by 0–100% relative to results for plain F-buffer, with xMAb1.1 showing the highest stabilization (100%) and MAb4.2 showing no stabilization at all (Table II). The general tendency is that antibodies that are stabilized by Tween 20 show similar or even higher stabilization in a medium. Only MAb1.3 and MAb1.7 tend to show slightly higher aggregation rates in a medium than in F-buffer containing Tween 20. The IgG4 MAb4.2 is an exception, because it is the only antibody that is not stabilized by Tween 20, at least not at the concentration used in the initial test (0.01%).

To identify an alternative compound that is suitable for stabilizing this antibody, we screened selected non-ionic and zwitterionic detergents, non-ionic polymers, sugars and arginine (Fig. 3b). MAb4.2 solutions in F-buffer were supplemented with the indicated compounds and stressed in the downscale stirring test (Fig. 3b). We found four additives that increased the MAb4.2 stability relative to plain F-buffer in an initial screening: Brij 35, PEG 4000, PEG 20000 and Poloxamer 188. Other compounds either did not influence MAb4.2 stability relative to Tween 20 (Triton X 100, CHAPS and Fos-Choline) or even decreased antibody stability (n-D-β-Maltopyranoside, Tween 80, Myristyl-sulfobetaine SB3-14, PEG 300, β-cyclodextrin, Methyl- β-cyclodextrin, trehalose, arginine). We repeated the stirring stress experiment, adding the 4 stabilizing compounds to the F-buffer in different concentrations (Fig. 3c). Within the concentration range used, the greatest stabilizing effect was achieved at the highest concentration (0.25%w/v) of all compounds except PEG 20000, and 0.25% (w/v) Poloxamer 188 (Pluronic F-68) provided the greatest degree of MAb4.2 stabilization. Under these conditions, the aggregation rate for MAb4.2 was 63% lower than in "unprotected" F-buffer. This lies well within the range of stabilization that was achieved with Tween 20 for the other 10 antibodies (Table II).

We then performed an additional bioreactor stress experiment to test the behavior of MAb4.2 in surfactant-supplemented F-buffer. MAb4.2 was stressed under the same conditions as those established for the bioreactor experiments described above, except that the F-buffer was supplemented with 0.2% (w/v) Poloxamer 188. Poloxamer 188 is a block polymer that is often used as a cell-protective agent in chemically defined media and in formulations of pharmaceutical proteins (34,35); CHO cells are known to grow in the presence of 0.2% (w/v) Poloxamer 188 (36).

As with all of our other bioreactor stress tests, we detected no product loss as indicated either by a decrease in SEC monomer peak area (Fig. 3d) or by UV absorption at 280 nm. Additionally, we found no increase in turbidity. The addition of antifoam did not increase turbidity; sparging with sterile air at 20 ccm/min likewise had no effect. Soluble aggregates increased by 1% until the end of the experiment, which is comparable to results from the stress test in F-buffer without Poloxamer 188.

In summary, adding surfactants to F-buffer in amounts commonly used in fermentation media yielded the same results under realistic fermentation-related stress conditions as similar stress tests in fermentation medium. Accordingly, the stabilizing effect observed in the fermentation medium can be explained by the presence of such substances in the formulation. An exception was the formation of soluble aggregates, which is significantly higher in the fermentation medium than in F-buffer with or without Poloxamer 188.

Chemical Modification of Antibodies Under Upstream Processing Conditions

Chemical Modification of Antibodies Under Conditions Relevant to Fermentation

In addition to stress-induced aggregation, fermentation conditions also run the risk of promoting a multitude of chemical modifications to antibodies, because the proteins are exposed to a complex chemical environment for a long period of time at an elevated temperature. Numerous modifications can be detected by charge-sensitive methods, since many reactions alter the electrostatic properties of surface residues (37). We established a protocol for analytical ion-exchange chromatography to quantify the changes of charge variants at different time points in the bioreactor stress experiments.

MAb4.2 samples already showed charge heterogeneity at time point t0, before the stress experiment was started (Fig. 4a). The main peak area at t0 was typically in the range of 75–80%, which decreased exponentially until the end of the experiment. This resulted in an increase in acidic forms, primarily three peaks with shorter retention times. The modifications that cause the emergence of these acidic peaks were analyzed by LC/MS (unpublished results). Peak 1 and peak 2 in Fig. 4a correspond to asparagine

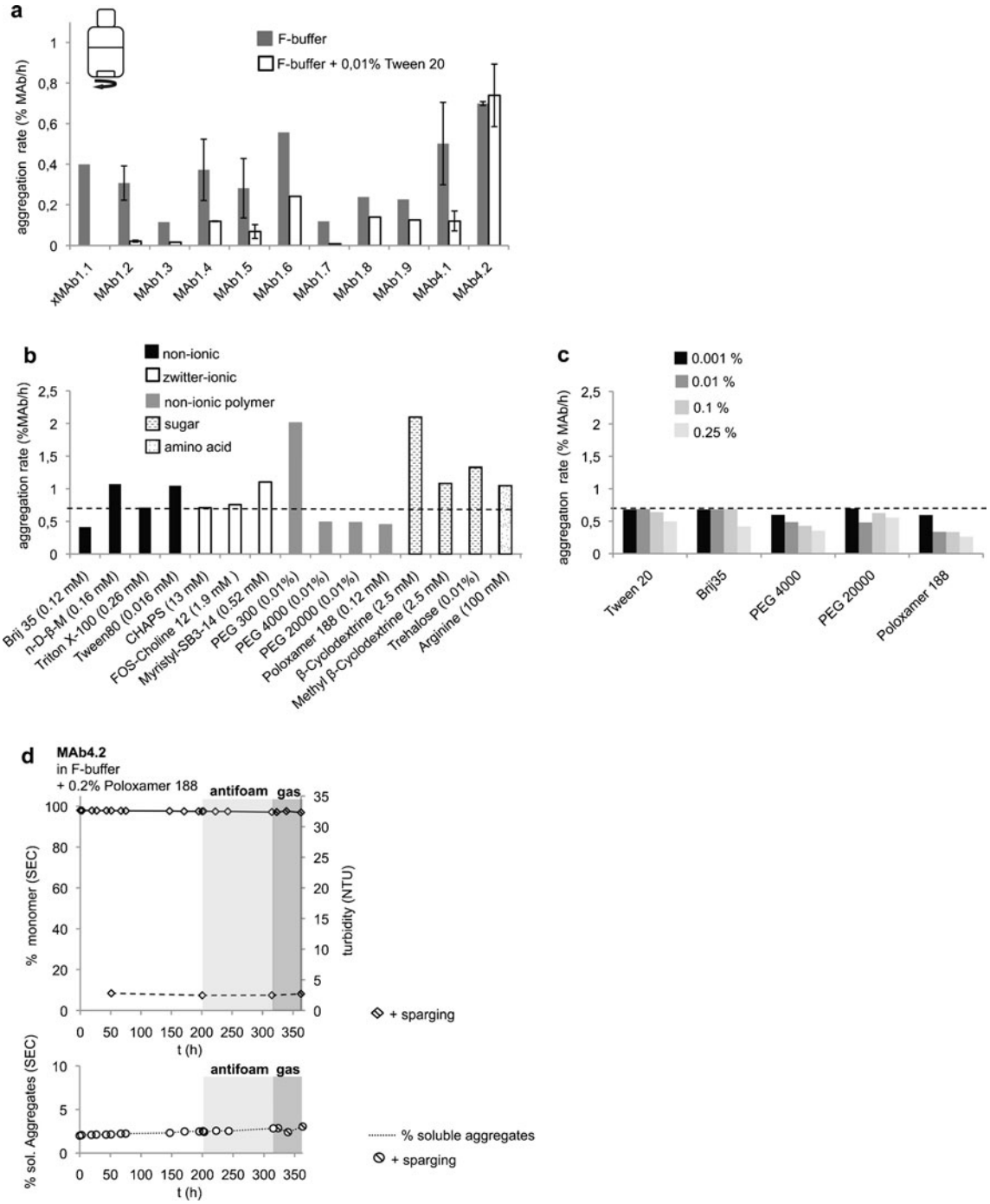

Fig. 3 Stabilization of MAb4.2 against aggregation in stirring stress. (**a**) Aggregation rates of 11 different antibodies stressed by stirring in the absence and presence of Tween 20. Aggregation rates in F-buffer are the same as in Fig. 1c. *Error bars* are indicated when multiple experiments were carried out: 5 (F-buffer) and 4 (F-buffer+0.01% Tween 20) experiments for MAb1.2; 2 and 2 experiments for MAb1.4; 2 and 2 experiments for MAb1.5; 2 and 2 experiments for MAb4.1; 4 and 6 experiments for MAb4.2. (**b**) Screening of 15 additives for reduction of the aggregation rate of MAb4.2 in F-Buffer. The compounds are grouped according to their substance class. The *dashed line* shows the aggregation rate of MAb4.2 in un-supplemented F-buffer from (a). When possible, the final concentration of each surfactant was calculated on the basis of its published critical micelle concentration (CMC, [41]) and normalized to 0.01% (w/v) Tween 20. All results are from single experiments. (**c**) Best stabilizing substances from (b) were tested again in single experiments in the concentrations indicated. The meaning of the dashed line is described in (b). (**d**) Stirring stress study of MAb4.2 in a 2 L bioreactor in F-buffer + 0.2% Poloxamer 188. "% Monomer (SEC)" and "% sol. aggregates (SEC)" are calculated as the corresponding relative peak areas of each chromatogram. Two experimental phases are indicated in *light gray* (addition of 0.05% (v/v) antifoam) and in *dark gray* (addition of 20 ccm/min sterile airflow).

deamidation in the CDR2. Peak 3 results from deamidation of an asparagine which is positioned in framework region 3.

The relative main peak areas at t0 were set to 100% and the decrease in the main peak was plotted against the

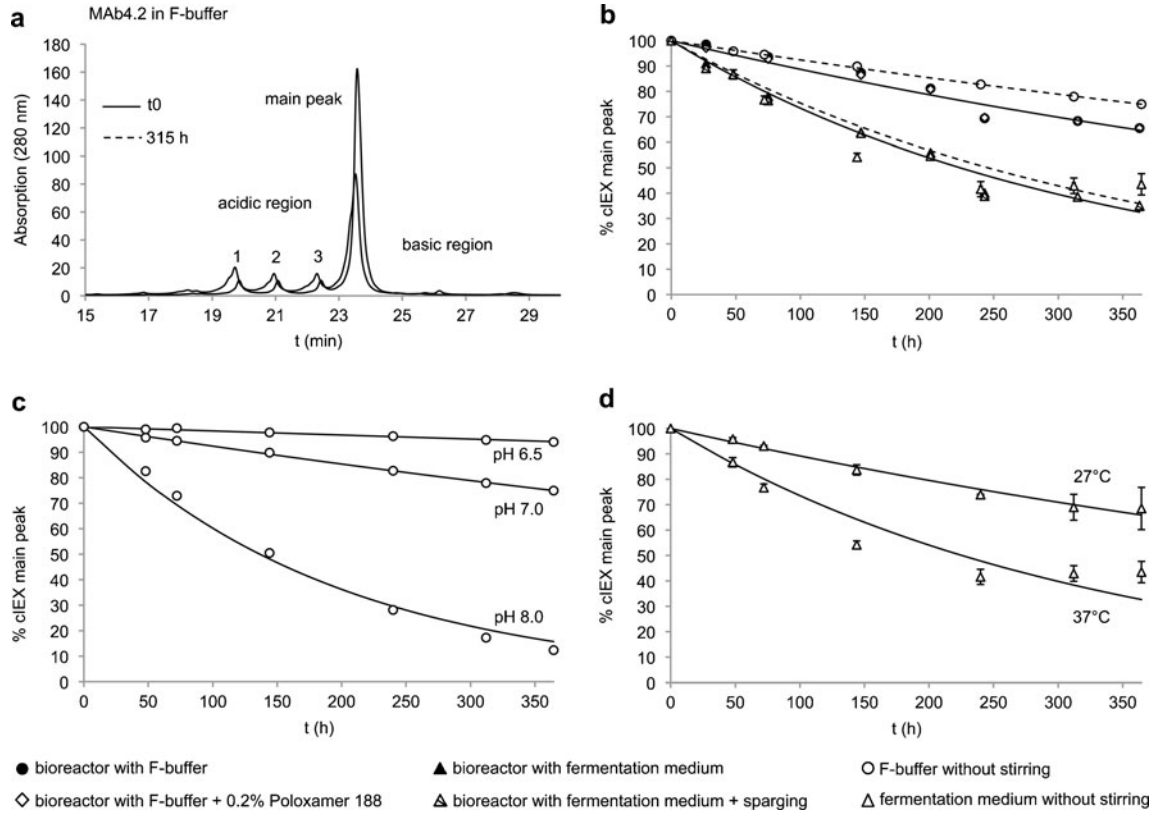

Fig. 4 Chemical modification of MAb4.2 stressed under conditions relevant to fermentation. (**a**) Cation exchange chromatograms of MAb4.2 from bioreactor stress samples. Two time points (0 h and 315 h) are shown to illustrate the decrease in the main peak and the increase in acidic species. (**b**) Decrease in the cIEX main peak in bioreactor stress tests samples. The main peak was integrated and is plotted as the fraction of total peak area of each chromatogram. The percentage of the main peak at time point t0 was set to 100%. *Solid* and *broken lines* show the fit to exponential decay curves for bioreactor stress samples and small samples incubated without stirring, respectively. Note that data from bioreactors with F-buffer +/- Poloxamer 188 are similar and datapoints do overlap. The same is true for data from bioreactors with medium +/- sparging. Data from bioreactors result from 1 experiment each, data from small scale stress samples that were not stirred result from 3 experiments. (**c**) Decrease in the cIEX main peak in F-buffer at different pH values without stirring. The values were obtained as described for (b) from downscale models. Solid lines show the fit to exponential decay curves. Each datapoint results from 3 parallel experiments. (**d**) Decrease in the cIEX main peak in the fermentation medium at different temperatures without stirring. The values were obtained as described for (b) and (c). *Solid lines* show the fit to exponential decay curves. Error bars result from 3 experiments.

experiment time (Fig. 4b–d). We fitted the resulting data to first-order exponential decay curves and used the derived rate constants for calculating the half-life of the main peak.

Calculated half-lives of the bioreactor stress samples were 578 h and 573 h in F-buffer and F-buffer+0.2% Poloxamer 188, respectively, 224 h in the unsparged fermentation medium and 221 h in sparged fermentation medium (Table III). Due to the large amount of antibody needed for single bioreactor stress tests, we were not able to conduct parallel experiments for statistical purposes. However, due to the highly similar modification rates observed in F-buffer and in the fermentation medium, we conclude that neither the presence of Poloxamer 188, nor sparging of the fermentation medium with sterile air had an impact on the extent of modification.

To determine whether sources of physical stress in the bioreactors (such as stirring and exposure to different

Table III cIEX Main-Peak Half-Lives Under Conditions Relevant to Fermentation

Condition	t½ MAb4.2 [h]
Bioreactor, F-buffer[a]	578
Bioreactor, F-buffer+0.2% Poloxamer 188[a]	573
Bioreactor, fermentation medium[a]	224
Bioreactor, sparged fermentation medium[a]	221
F-buffer, pH7.0 (37°C)[b]	877
F-buffer, pH6.5 (37°C)[b]	4219
F-buffer, pH8.0 (37°C)[b]	137
Fermentation medium (CD CHO) 37°C[b]	226
Fermentation medium (CD CHO) 27°C[b]	606
In-house fermentation medium 37°C[b]	229

[a] Samples from bioreactor stress experiments

[b] Samples from downscale stress test without stirring

surfaces) has an influence on the observed modification rates, we analyzed MAb4.2 samples that had been incubated in F-buffer and in the medium at 37°C without agitation (Fig. 4b, dashed lines). For these samples, the cIEX main-peak half-life values are 1.5-fold higher (877 h) in F-buffer and similar (226 h) in the fermentation medium when compared to values obtained in bioreactors.

To test the influence of fermentation medium compounds on the cIEX main peak decrease, we modified the F-buffer by adding components that could potentially be responsible for the higher rate observed in the medium. We prepared formulations of MAb4.2 in F-buffer with varying glucose concentrations but observed no change in the extent of modification (data not shown). Glycation is therefore not a driver of the modification observed in F-buffer. Furthermore, we tested the influence of vitamin and trace element solutions that are added to the medium, but detected no impact on the extent of modification (data not shown). Additionally, we formulated the antibody in F-buffer at various pH levels and checked the influence of temperature on modification kinetics as well. As seen in Fig. 4c, an increase in pH accelerates the modification of MAb4.2. At a pH of 6.5 the main-peak half-life is significantly increased (4291 h, which is 4.8-fold higher than at pH 7.0). Consequently, the half-life decreases at pH 8.0 (137 h, which is 6.4-fold lower than at pH 7.0).

Figure 4d shows the influence of temperature on the modification rate. MAb4.2 was incubated in the fermentation medium at 27°C and compared to the cIEX main peak decrease observed at 37°C. The modification rate was significantly diminished at the lower temperature, with the cIEX main-peak half-life increasing 2.7-fold to 606 h.

In summary, we found that MAb4.2 is chemically modified under fermentation-relevant stress conditions. Analytical cation exchange chromatography shows that these modification(s) result(s) mainly in a shift to acidic forms, which means that the molecules either lose positive charge and/or gain negative charge. We were able to rule out glycation and the involvement of vitamins and trace elements in the fermentation medium as a cause for this observation but were also able detect a strong pH and temperature dependency, resulting in higher modification rates at more basic pH and higher temperatures. The formation of acidic isoforms and the powerful effect of pH and temperature is well known for deamidation reactions (38) and is confirmed by the finding that deamidated asparagine residues in the acidic peaks grew during stress exposure.

Chemical Modification of Antibodies in Real Cell Culture Fermentations

Conditions and kinetics in real cell culture fermentations are more complex than that observed in small-scale stress models as well as in large-scale bioreactor stress tests. In real fermentations, antibodies are not continuously exposed to fermentation stress conditions, because cell density increases during fed-batch fermentation and thus new and unmodified antibodies are delivered during the different phases of a fermentation. When these newly synthesized molecules are added to a pool of antibodies, the degree of modification varies according to their individual residence times in the cell culture broth. In addition, the composition of the medium changes continuously, because cells consume medium constituents and produce metabolites that are released into the medium. Especially in late phases of a fermentation, a decrease in cell viability can lead to increased cell lysis, which modifies the fermentation broth as well.

To obtain a realistic view of antibody modification during real cell culture fermentations, we analyzed MAb4.2 over the course of three CHO cell culture fermentations. The bioreactors in which these experiments were carried out were similar to those used for the stress experiments described above, except that the former utilized an in-house medium platform. We performed small-scale stress tests to determine whether modification rates in this medium are different from those observed in the CD CHO medium. The calculated cIEX main-peak half-life for MAb4.2 was 229 h (data not shown) in the in-house fermentation medium at 37°C, making it similar to the rate observed in commercial medium (226 h, Table III).

During the MAb4.2 fermentations, samples were withdrawn from the bioreactors at the time points indicated in Fig. 5a and analyzed for product concentration, cell viability and charge heterogeneity. Figure 5a shows one of the three fermentations as an example. During the initial phase (up to day 4), viable cell density remains low and only minor amounts of antibody are produced. From day 4 to day 8, the viable cell count increases exponentially with a peak at day 8. The production rate (new product/day) increases during this phase as well. After day 8, the production rate stays at a constant level until day 10 when it decreases together with the viable cell density until the end of the fermentation. As a consequence, the shape of the total product concentration curve is sigmoidal.

When analyzing the resulting modification, we excluded data from t0 to day 3 when the fermentation antibody titers are too low to allow for an accurate determination of the antibody charge heterogeneity. As a measure for the degree of MAb4.2 modification after day 4, we used the percentage of the main peak area with respect to the integrated total peak area of the chromatograms at a given time point. This approach was chosen because no starting value (100%) was available in this experiment (unlike the stress experiments described above).

A relative cIEX main peak area of 90% can be seen at day 4, which means that 10% of the molecules produced in

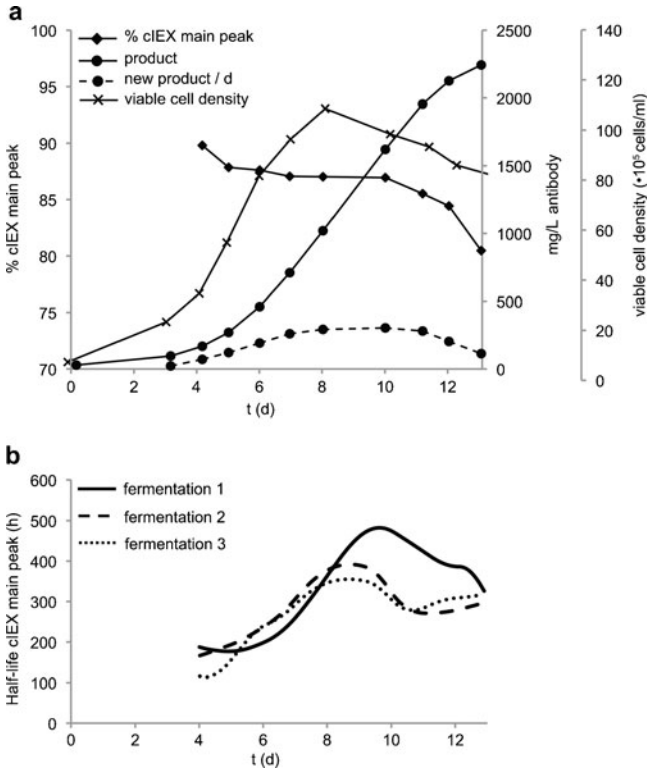

Fig. 5 Chemical modification of MAb4.2 in real fed batch cell culture fermentations. (**a**) Plots of product concentration, production rate, viable cell density and chemical modification in one of the three MAb4.2 fermentations. (**b**) Plots of modification rates over the course of three MAb4.2 fermentations expressed as cIEX main-peak half-life. The values were calculated as described in the Results section. Fermentation 1 corresponds to the data shown in (a).

the first 4 days of fermentation were modified. The relative main peak area stays constant from day 5 to day 10, which correlates to an increase in the production rate, because unmodified molecules contributing to the main peak are released into the medium and compensate for the formation of modified species. A reduction in relative main peak area is detectable from day 10 on, when the overall production rate starts to decrease. In this phase, the delivery of unmodified antibodies goes down and no longer compensates for the modification reaction(s). A relative main peak area of 80% was measured at the end of the fermentation, which means that one fifth of the product was chemically modified. The 80% main peak fits well with the charge heterogeneity observed for the purified starting material used for the bioreactor stress tests (see above). The overall charge heterogeneity of purified MAb4.2 is clearly generated during fermentation and carried over to the purified product. Downstream conditions usually do not generate or remove significant amounts of the major charged isoforms that are present in the cell culture harvest.

Analysis of Modification Rates in Real Cell Culture Fermentations

We initially tried to fit experimental fermentation data to formation rates of new product and to the kinetics of the deamidation reaction, as determined in a downscale model with medium. Deviations of the calculated and the measured main peak curves indicated that additional parameters may have an effect on the modification reaction. We then calculated the modification rates during different phases of the fermentation based on the experimental data. We considered the following parameters: the relative peak area $\mathcal{N}(t)$ is affected by both the modification rate and the production of new unmodified product. The following summary equation provides a good approximation of this for discrete time intervals:

$$\mathcal{N}[t_i] = \frac{C[t_{i-1}]}{C[t_i]} * \mathcal{N}[t_{i-1}] * e^{k[t_i]*(t_i - t_{i-1})} + \left(1 - \frac{C[t_{i-1}]}{C[t_i]}\right) * 100 \tag{1}$$

where $\mathcal{N}[t_{i\text{-}1}]$ and $\mathcal{N}[t_i]$ are the relative peak areas measured at two consecutive times $t_{i\text{-}1}$ and t_i. $C[t_{i\text{-}1}]$ and $C[t_i]$ are the product concentrations at the same two time points, and $k[t_i]$ is the modification rate in the time interval from $t_{i\text{-}1}$ to t_i. The bracket notation $[t_i]$ indicates that we indeed only have a formula in the discrete case. This equation was converted to the following formula, which estimates the modification rate for the given time interval:

$$k[t_i] = \log\left(\frac{\mathcal{N}[t_i] - \left(1 - \frac{C[t_{i-1}]}{C[t_i]}\right) * 100}{\frac{C[t_{i-1}]}{C[t_i]} * \mathcal{N}[t_{i-1}]}\right) / (t_i - t_{i-1}) \tag{2}$$

Calculations such as this are heavily influenced by the length of time between two consecutive measurements and by the rate at which product concentration and relative peak area change in the time interval. It is also reasonable to assume that new product is immediately susceptible to modification. To accommodate for this and to obtain a more realistic approximation of the continuous modification rate $k(t)$, we introduced a preprocessing step. First we fitted "splines" (piecewise-polynomial functions) to our product concentration and relative peak area measurements. This means that the data are split into intervals and polynomial functions—cubic functions in this case—are fitted onto the data. We then used these to predict artificial measurements at 84 different time points over the time frame of the given fermentation, an approach that simulates measurements at roughly every 4 h. We used these data to calculate the modification rate with formula (2) and converted the results into main-peak half-lives as described in Materials and Methods (Fig. 5b). Our calculations show that at day 4 of

fermentation, the main-peak half-lives of the three fermenters range between 115 h and 190 h. Unexpectedly, half-lives increase in all three fermentations until day 9–10. After this period, half-life values decrease again, but seem to stay at a rather constant level until the end of the fermentation. Interestingly, progressions of the modification rates seem to correlate with the course of the production rate and viable cell density. Main-peak half-lives increase during the exponential phase of viable cell density when the production rate likewise increases until day 9 and then slightly decrease during the last 4 days of cultivation. The overall magnitude of main-peak half-life correlates to the value we obtained (229 h) by incubating MAb4.2 in the in-house medium. In our calculated curves, a main-peak half-life of 229 h is reached between day 5 and day 7 in the three fermentations.

In summary, the modifications we detected in MAb4.2 in cell culture fermentations were the same as those in the stress experiments. Unexpectedly, calculated modification rates were not constant throughout the course of the fermentations.

DISCUSSION

Aggregation in Downscale Models and Bioreactors

Antibodies are highly homologous in sequence and structure and usually exhibit a high degree of thermal stability well above 60°C (28,39). Surprisingly, we detected that the behavior of our panel of 11 antibodies varied considerably under stirring and shaking stress, despite a high similarity in sequence. For example, the least stable antibody under stirring stress (MAb4.2) and the most stable molecule under the same conditions (MAb1.3) show a sequence identity of 80% for the heavy chain and 92% for the light chain. In addition, these two molecules also behave completely different to stabilization by Tween 20 (Table II). This underscores our findings that the response of a molecule to certain conditions cannot necessarily be used as a model for other molecules of highly similar sequence and structure.

In another study using a similar downscale stirring stress model, aggregation of a monoclonal IgG1 antibody (which was not part of this study) was detected in the presence and absence of Tween 20 (21). Stirring for 168 h (25°C, pH6.0, 10 mg/mL) resulted in a 34% product loss, which corresponds to an aggregation rate of 0.2% MAb/h. This lies well within the rates observed for those of our antibodies that were stressed under slightly different conditions. The presence of 0.05% Tween 20 reduced the aggregation rate by 75%, which is again within the range of stabilization efficiency that we found, albeit at a lower Tween 20 concentration (Table II).

Our results also confirm published data that show stirring stress to be more intense than shaking stress (21,23). Only one of the 5 antibodies we tested was found to be less stable under shaking stress than under stirring stress (MAb1.5), while the other 4 were significantly more stable. Under shaking stress conditions, we were able to detect the formation of soluble aggregates, which we did not observe in stirred samples. Not all of the 5 antibodies tested were similarly susceptible towards this aggregation pathway: only xMAb1.1 showed a considerable increase in dimer and oligomer species (8.8%) within 72 h of shaking stress, whereas MAb1.8 and MAb4.2 exhibited lower levels. Interestingly, soluble aggregates were reduced in medium, except for MAb4.2 . Thus, MAb4.2 does not respond to a stabilizing effect by medium components that obviously protect the other two antibodies against the formation of soluble aggregates.

Stability in the stirring stress experiments was not predictive of behavior under shaking stress and vice versa. The aggregation rate of MAb4.2, for example, was 7.8 times higher under stirring stress than under shaking stress, whereas MAb1.5 was 2.6 times more unstable under shaking stress. Moreover, it was shown that stirring and shaking stress produce different aggregate species, qualitatively as well as quantitatively (21,23). This means that antibodies exhibit a highly versatile response towards different kinds of physical stress which is determined by distinct aggregation pathways.

We were not able to fully correlate the thermal stability of the antibodies (T_{agg} obtained by DLS and T_m obtained by DSC) to their stability towards stirring or shaking stress. The onset of aggregation (T_{agg}) for the 11 antibodies was in general not predictive for their stability in F-buffer and medium when challenged by stirring or shaking. In contrast to that, the transition temperatures we measured by differential scanning calorimetry for 3 of the antibodies reflected their stabilities in the downscale stirring models, but not those of the downscale shaking models. In general T_{agg} and T_m values are ≥60°C for most of the antibodies which suggests that thermal instability is not the main driver of aggregation in our stress models at 37°C. In line with this, it is known from literature that the thermal stability of a protein does not necessarily correlate with its tendency to aggregate (40,41). Recently, the analysis of the pH and temperature stability of 77 antibodies by King *et al.* (42) likewise failed to show any correlation of these parameters.

We found that the T_{agg} as well as the T_m was in general slightly lower in medium than in buffer (Table II), suggesting destabilization by medium components, which did not correlate to the observations from the downscale stirring and shaking stress experiments. Similar observations were made for human growth hormone, which was stabilized towards agitation-induced damage upon the addition of

Tween 20, but differential scanning calorimetry showed a decrease in the melting temperature by 2°C (32). Formulation components such as polyols were also shown to have non-correlating effects on the thermal and mechanical stability of antibodies (43). It follows that the higher stability observed in the stirring and shaking experiments in medium seems to be related to a stabilization mechanism that does not increase aggregation temperatures.

The high tendency of some antibodies to aggregate when exposed to different kinds of mixing raises the question as to whether this is also true during fermentation, since stirring and turnover of the gas/liquid interface are predominant challenges for the proteins within a bioreactor. The large impact of the mixing mechanism on antibody stability is substantiated in a further downscale model: the aggregation rates measured with the small scale "top-stirrer" devices were significantly lower than with the "bottom-stirrer" vessels. Since the dimensions and physical parameters like the Reynold's number of these experiments were identical, we explain the observed differences primarily by the stirring method. The higher stress in the "bottom stirrer" vessels seems to be mainly imposed by the friction between the stirrer bar and the glass surface. Additionally, an altered local turbulent movement of the fluid imposed by a difference in the position of the stirrer might also have an impact. It is already known from literature, that "bottom-stirrer" systems impose higher stress on antibody solutions compared to "top-stirrer" systems (27).

In general, the "top-stirrer" downscale model might be a better approximation towards stress in a real bioreactor because of the more similar stirring methods. Nevertheless, it does not completely reproduce real physical stress in a bioreactor which is shown by the difference in the Reynold's number of both systems. The Re of the bioreactor is ~12.5 times higher compared to the downscale stirring models, indicating turbulent fluid dynamics for the large system and non-turbulent dynamics for the smaller ones. Because of these shortcomings we conducted a stress experiment in real bioreactors to analyze the stability of antibody molecules under realistic conditions. For this, we selected MAb4.2, which exhibited the most interesting behavior in our downscale stress models: First, under stirring stress MAb4.2 displayed the highest aggregation rates in buffer as well as in medium. Second, soluble aggregates induced in shaking stress were not reduced by medium components.

Aggregation of MAb4.2 in bioreactors was clearly less pronounced than in the downscale stress experiments. No product loss was detected in F-buffer and in medium, only an increase in solution turbidity in F-buffer revealed residual aggregation. This was increased by the additional stress of sparging, but not by the addition of antifoam. In medium, MAb4.2 was fully protected against any sign of aggregation, as turbidity did not increase even if the solution was sparged. Again, a measurable stabilizing effect by medium components was eminent which mirrors the results in the small scale stress tests.

Surfactants are used in medium formulations in concentrations that are comparable to those used for stabilizing purified proteins, and their primary purposes are to protect cells from shear stress and to ensure that insoluble compounds such as vitamins and fatty acids disperse effectively (44,45). This makes these substances candidates for the protective effects we observed. The mechanism by which surfactants stabilize against aggregation is usually described in terms of competition between surfactant and protein for the absorption to hydrophobic surfaces and/or to the gas/-liquid interface (46). This absorption is achieved through thermodynamic stabilization (45) or through the binding of surfactant molecules to exposed hydrophobic regions of partially denatured proteins (32). Adding Tween 20 at a concentration of 0.01%, which can be found in cell culture medium formulations (44) and in drug product formulations (21,31,32) allowed us to significantly stabilize 10 out of 11 antibodies against stirring-induced aggregation. MAb4.2, which was not responsive to Tween 20, could be stabilized using Poloxamer 188, another compound primarily used in medium formulation for cell protection (35,47). When used at a concentration that is realistic for fermentation media, Poloxamer significantly stabilized MAb4.2 under downscale stirring stress as well as under bioreactor conditions. Thus, we attribute the stabilizing effects of fermentation medium towards aggregation induced by physical stress to the presence of surfactants.

However, such medium components did not prevent soluble MAb4.2 aggregates from forming, as had already been seen in downscale shaking stress. An increase of 4.5% and 5.9% of soluble dimers and oligomers in unsparged and sparged bioreactors, respectively, was detected by SEC over the course of 363 h of experimental time. These values lie well within the range of the soluble aggregate amounts that are detected in the harvests of antibody fermentations (3). By comparison, soluble aggregates increased by 1.6% within 72 h under downscale stress in medium, which is comparable to the rate in the sparged bioreactor. Unexpectedly, soluble aggregates were not found to increase significantly in the bioreactor stress experiment with F-buffer, which contradicts the formation of 1.9% within 72 h in the small-scale shaking experiment. This indicates that the behavior of MAb4.2 in the downscale shaking setup does not fully represent its behavior under realistic conditions. Moreover, the fact that MAb4.2 forms soluble aggregate in bioreactors with medium but not with buffer suggests that medium components destabilize the antibody with respect to this aggregation pathway.

Chemical Modification of Antibodies

Long term stability of antibody therapeutics usually is improved by slightly acidic pH and low storage temperature (11,48,49 and references therein). In contrast, typical fed batch fermentations of mammalian cells are usually carried out for 2 weeks at a near neutral pH and a physiological temperature of 37°C. These values are beneficial for the progression of deamidation reactions, but at the same time they cannot be optimized to slow down deamidation rates, since they are mandatory for optimal cell growth and protein expression. Indeed, MAb4.2 was rapidly deamidated under stress conditions simulating fermentation as well as in real cell culture fermentations.

We measured a pH- and temperature-dependent increase in charge heterogeneity represented by a reduction in the unmodified cIEX main peak when MAb4.2 antibody solutions were stressed in bioreactors. One of the modifications we observed was deamidation in one of the CDR regions. Although this has no impact on the function of our model antibody (data not shown), deamidation within CDRs can result in reduced target binding and potency (50). We observed a higher modification rate in the fermentation medium than in the buffer, and primarily attribute this effect to the pH of the medium, which was more basic than that of the F-buffer (7.3 and 7.0, respectively). In addition, ionic strength and buffer components are also known to influence the speed of deamidation reactions (51), which might account for the observed differences. Physical parameters of the bioreactor setup do not seem to drive deamidation reactions, as modification rates in bioreactors were comparable to those obtained from experiments in which MAb4.2 was incubated under the same conditions without additional physical stress.

Modifications detectable by analytical cIEX in real cell culture fermentations were identical to those in stress experiments, but the corresponding kinetics are markedly different. This is due to the fact that within each time interval, newly produced, unmodified molecules in cell cultures are secreted by cells at different rates, because the density of viable, protein-secreting cells and the specific productivity of these cells change during fermentation. The synthesis of "fresh" molecules compensates for the modification kinetics up to day 10 of cell culture, and the portion of the main peak in cIEX stays at ~85%. In the later phase of fermentation, the proportion of newly synthesized molecules decreases and can no longer counterbalance the modification reactions. Accordingly, reduction of the main peak increases from day 10 to 13. Progressive deamidation of a monoclonal antibody in a CHO cell culture was reported, as was the appearance of new charge variants, which was associated with a major decrease in cell viability over the last 4 days of fermentation (52). In our example in Fig. 5, cell viability only decreases slowly after day 8 and still is very high at the end of the process on day 13, while the main-peak curve starts to decrease at day 10. Obviously, cell viability alone is not sufficient to indicate significant changes in product quality.

Surprisingly, modification rates are not constant during cell culture fermentations of MAb4.2. While the magnitude of the estimated main-peak half-lives at neutral pH are comparable to those we measured in bioreactor stress experiments (220 h–230 h, Table III), calculated values range between 113 h and 482 h in the three MAb4.2 fermentations we evaluated, which corresponds to a factor of 0.5–2.1 (Fig. 5b). Although the calculated curves show considerable deviations when the three fermentations are compared, the overall trend seems to correlate with the different fermentation phases in each experiment: first, the main-peak half-life increases (the modification rate decreases) during the exponential phases of protein production and cell growth, while it ceases together with the production rate and viable cell density in the late phase of cell culture. This variability is not explainable by changes in pH or in temperature, since these parameters were constant throughout the fermentations. However, the consumption of medium constituents and the production of metabolites by cells, as well as the addition of feeds during the fermentation process continuously alter the conditions in the fermentation broth. Identifying parameters that influence modification speed could lead to solutions for controlling modification rates in order to obtain a more homogenous product. Fermentation strategies and harvest criteria focusing only on achieving high titers and yields without considering the possible effect of extended culture times on product quality may result in reduced and varying quality of the product.

In vivo deamidation of an antibody was shown with a half-life of 140 h for a single deamidation site (53), and, interestingly, *in vivo* deamidation rates are similar to the rates *in vitro* (54). Since a cell culture closely resembles *in vivo* conditions, an antibody that is modified at a certain rate in a cell culture will probably exhibit comparable behavior when applied in a patient, regardless of its stable storage formulation. Therefore, the USP stability of an antibody in cell culture is predictive for the *in vivo* stability of an antibody and early characterization of product modifications can identify potential problems in the further development of a therapeutic protein.

CONCLUSIONS

This study has investigated the stability of antibodies under conditions relevant to upstream processing, with a focus on aggregation and chemical modification. Our results show

the difficulty of predicting and generalizing the behavior of antibodies under such conditions. First, the sensitivity of these highly homologous proteins under process relevant stress conditions is highly diverse, which makes it difficult to make assumptions based on the behavior of a model molecule. Second, small scale stress models are limited in their ability to predict stress on a realistic scale because the least stable of the molecules we tested in downscale stirring stress models did not show significant aggregation in a bioreactor. Third, different aggregation pathways are influenced differently by medium components. For example, formation of MAb4.2 HMW aggregates was suppressed in fermentation medium, whereas the same condition allowed for the formation of soluble aggregates. In general our results suggest, that product loss by precipitation is not a major concern during fermentation and we identified surfactants, such as Tween 20 and Poloxamer 188, as medium constituents that are responsible for stabilization. Soluble aggregates often occur in antibody fermentation harvests. We found that such oligomers emerge in fermentation media in bioreactors at rates comparable to those in small-scale shaking stress experiments. Thus, the use of small-scale shaking stress tests should be considered as a means of testing substances that inhibit this aggregation pathway in problematic cases. It is noteworthy that the stability of the novel CrossMab in our stirring and shaking stress models was within the range observed for regular IgG1formats. As this bispecific molecule was designed to structurally resemble an IgG1 antibody, this confirms that the new format fully retains the structural properties that are important for stability.

We also investigated the kinetics of chemical modifications to an antibody during fermentation. Extensive deamidation was detected in stress models and was even more pronounced in real cell culture fed batch fermentations. We showed that product heterogeneity at the end of a fermentation is mainly a function of the modification rate and the rate at which new product is secreted to the fermentation medium. Cell lysis, medium component metabolism and conditioning of the medium with feeds seem to slightly modify the reaction rates. Monitoring product quality during cell culturing is therefore even more important than product titer for optimizing the fermentation process design and defining harvest criteria to ensure constant high product quality. Finally, the kinetics of chemical modification of antibodies in cell culture is comparable to that in serum. Thus, chemical stability data from cell culture can be used to predict potential stability problems very early in the development of therapeutic molecules.

ACKNOWLEDGMENTS AND DISCLOSURES

We would like to thank Carolin Lucia and Katharina Didzus from Roche Penzberg for their support with bioreactor stress experiments, Sabrina Mahlack for her support with MAb4.2 purification, and Hubert Kettenberger, Holger Kley and Xaver Reiser for their support with DLS and DSC measurements. We would also like to thank Alexandra Schindl for carrying out the shaking stress experiments and Robert Puskeiler for support with calculations of physical parameters of the stirring stress models.

We are also grateful to Jörg Hörnschemeyer and Jonas Fast of Roche Basel for sharing information about the identity of cIEX peaks.

S.D, F.H. F.L. O.P. and K.L are all employees of Roche at the time of publication. The remaining authors declare no competing financial interests.

REFERENCES

1. Carter PJ. Potent antibody therapeutics by design. Nat Rev Immunol. 2006;6:343–57.
2. Schaefer W, Regula JT, Bähner M, Schanzer J, Croasdale R, Dürr H, Gassner C, Georges G, Kettenberger H, Imhof-Jung S, Schwaiger M, Stubenrauch KG, Sustmann C, Thomas M, Scheuer W, Klein C. Immunoglobulin domain crossover as a generic approach for the production of bispecific IgG antibodies. Proc Natl Acad Sci USA. 2011;108(27):11187–92.
3. Cromwell MEM, Hilario E, Jacobson F. Protein aggregation and bioprocessing. AAPS J. 2006;8:E572–9.
4. Vazquez-Rey M, Lang DA. Aggregates in monoclonal antibody manufacturing processes. Biotechnol Bioeng. 2011;108:1494–508.
5. Schroder M, Schafer R, Schafer R, Friedl P. Induction of protein aggregation in an early secretory compartment by elevation of expression level. Biotechnol Bioeng. 2002;78:131–40.
6. Zhang YB, Howitt J, McCorkle S, Lawrence P, Springer K, Freimuth P. Protein aggregation during overexpression limited by peptide extensions with large net negative charge. Protein Expr Purif. 2004;36:207–16.
7. Nakanishi K, Sakiyama T, Imamura K. On the adsorption of proteins on solid surfaces, a common but very complicated phenomenon. J Biosci Bioeng. 2001;91:233–44.
8. Franco R, Daniela G, Fabrizio M, Ilaria G, Detlev H. Influence of osmolarity and pH increase to achieve a reduction of monoclonal antibodies aggregates in a production process. Cytotechnology. 1999;29:11–25.
9. Arosio P, Barolo G, Muller-Spath T, Wu H, Morbidelli M. Aggregation stability of a monoclonal antibody during downstream processing. Pharm Res. 2011;28:1884–94.
10. Biddlecombe JG, Craig AV, Zhang H, Uddin S, Mulot S, Fish BC, Bracewell DG. Determining antibody stability: creation of solid–liquid interfacial effects within a high shear environment. Biotechnol Prog. 2007;23:1218–22.
11. Wang W, Singh S, Zeng DL, King K, Nema S. Antibody structure, instability, and formulation. J Pharm Sci. 2007;96:1–26.
12. Rosenberg AS. Effects of protein aggregates: an immunologic perspective. AAPS J. 2006;8:E501–7.
13. Vazquez E, Corchero JL, Villaverde A. Post-production protein stability: trouble beyond the cell factory. Microb Cell Fact. 2011;10:10–60.
14. Gomez N, Subramanian J, Ouyang J, Nguyen MD, Hutchinson M, Sharma VK, Lin AA, Yuk IH. Culture temperature modulates aggregation of recombinant antibody in cho cells. Biotechnol Bioeng (2011).

15. Quan C, Alcala E, Petkovska I, Matthews D, Canova-Davis E, Taticek R, Ma S. A study in glycation of a therapeutic recombinant humanized monoclonal antibody: where it is, how it got there, and how it affects charge-based behavior. Anal Biochem. 2008;373:179–91.
16. Li S, Schoneich C, Borchardt RT. Chemical instability of protein pharmaceuticals: mechanisms of oxidation and strategies for stabilization. Biotechnol Bioeng. 1995;48:490–500.
17. Liu H, Gaza-Bulseco G, Faldu D, Chumsae C, Sun J. Heterogeneity of monoclonal antibodies. J Pharm Sci. 2008;97:2426–47.
18. Geiger T, Clarke S. Deamidation, isomerization, and racemization at asparaginyl and aspartyl residues in peptides. Succinimide-linked reactions that contribute to protein degradation. J Biol Chem. 1987;262:785–94.
19. Kim JY, Lee GM. CHO cells in biotechnology for production of recombinant proteins: current state and further potential. Appl Microbiol Biotechnol. 2012;93(3):917–30.
20. Becker E, Florin L, Pfizenmaier K, Kaufmann H. An XBP-1 dependent bottle-neck in production of IgG subtype antibodies in chemically defined serum-free Chinese hamster ovary (CHO) fed-batch processes. J Biotechnol. 2008;135:217–23.
21. Kiese S, Papppenberger A, Friess W, Mahler HC. Shaken, not stirred: mechanical stress testing of an IgG1 antibody. J Pharm Sci. 2008;97:4347–66.
22. Ridgway JB, Presta LG, Carter P. 'Knobs-into-holes' engineering of antibody CH3 domains for heavy chain heterodimerization. Protein Eng. 1996;9:617–21.
23. Mahler HC, Muller R, Friess W, Delille A, Matheus S. Induction and analysis of aggregates in a liquid IgG1-antibody formulation. Eur J Pharm Biopharm. 2005;59:407–17.
24. Pace CN, Vajdos F, Fee L, Grimsley G, Gray T. How to measure and predict the molar absorption coefficient of a protein. Protein Sci. 1995;4:2411–23.
25. Maa YF, Hsu CC. Protein denaturation by combined effect of shear and air-liquid interface. Biotechnol Bioeng. 1997;54:503–12.
26. Thomas CR, Geer D. Effects of shear on proteins in solution. Biotechnol Lett. 2011;33:443–56.
27. Ishikawa T, Kobayashi N, Osawa C, Sawa E, Wakamatsu K. Prevention of stirring-induced microparticle formation in monoclonal antibody solutions. Biol Pharm Bull. 2010;33:1043–6.
28. Heads JT, Adams R, D'Hooghe LE, Page MJT, Humphreys DP, Popplewell AG, Henry AJ. Relative stabilities of IgG1 and IgG4 Fab domains: influence of the light-heavy interchain disulfide bond architecture. Protein Sci. 2012;21:1315–22.
29. Ionescu RM, Vlasak J, Price C, Kirchmeier M. Contribution of variable domains to the stability of humanized IgG1 monoclonal antibodies. J Pharm Sci. 2008;97:1414–26.
30. Li F, Vijayasankaran N, Shen AY, Kiss R, Amanullah A. Cell culture processes for monoclonal antibody production. MAbs. 2010;2:466–79.
31. Chou DK, Krishnamurthy R, Randolph TW, Carpenter JF, Manning MC. Effects of Tween 20 and Tween 80 on the stability of Albutropin during agitation. J Pharm Sci. 2005;94:1368–81.
32. Bam NB, Cleland JL, Yang J, Manning MC, Carpenter JF, Kelley RF, Randolph TW. Tween protects recombinant human growth hormone against agitation-induced damage via hydrophobic interactions. J Pharm Sci. 1998;87:1554–9.
33. Bahrami A, Shojaosadati SA, Khalilzadeh R, Mohammadian J, Farahani EV, Masoumian MR. Prevention of human granulocyte colony-stimulating factor protein aggregation in recombinant Pichia pastoris fed-batch fermentation using additives. Biotechnol Appl Biochem. 2009;52:141–8.
34. Chisti Y. Animal-cell damage in sparged bioreactors. Trends Biotechnol. 2000;18:420–32.
35. Clincke MF, Guedon E, Yen FT, Ogier V, Roitel O, Goergen JL. Effect of surfactant pluronic F-68 on CHO cell growth, metabolism, production, and glycosylation of human recombinant IFN-gamma in mild operating conditions. Biotechnol Prog. 2011;27:181–90.
36. Gigout A, Buschmann MD, Jolicoeur M. The fate of Pluronic F-68 in chondrocytes and CHO cells. Biotechnol Bioeng. 2008;100:975–87.
37. Vlasak J, Ionescu R. Heterogeneity of monoclonal antibodies revealed by charge-sensitive methods. Curr Pharm Biotechnol. 2008;9:468–81.
38. Zheng JY, Janis LJ. Influence of pH, buffer species, and storage temperature on physicochemical stability of a humanized monoclonal antibody LA298. Int J Pharm. 2006;308:46–51.
39. Vermeer AW, Norde W. The thermal stability of immunoglobulin: unfolding and aggregation of a multi-domain protein. Biophys J. 2000;78:394–404.
40. Wang W, Nema S, Teagarden D. Protein aggregation–pathways and influencing factors. Int J Pharm. 2010;390:89–99.
41. Schaefer JV, Pluckthun A. Engineering aggregation resistance in IgG by two independent mechanisms: lessons from comparison of Pichia pastoris and mammalian cell expression. J Mol Biol. 2012;417:309–35.
42. King AC, Woods M, Liu W, Lu Z, Gill D, Krebs MR. High-throughput measurement, correlation analysis, and machine-learning predictions for pH and thermal stabilities of Pfizer-generated antibodies. Protein Sci. 2011;20:1546–57.
43. Abbas SA, Sharma VK, Patapoff TW, Kalonia DS. Opposite effects of polyols on antibody aggregation: thermal *versus* mechanical stresses. Pharm Res. 2012;29:683–94.
44. Cartaya OA. Serum-free cell culture media. United States Patent 4,205,126, 1980.
45. Wang W. Instability, stabilization, and formulation of liquid protein pharmaceuticals. Int J Pharm. 1999;185:129–88.
46. Randolph TW, Jones LS. Surfactant-protein interactions. Pharm Biotechnol. 2002;13:159–75.
47. van der Pol L, Tramper J. Shear sensitivity of animal cells from a culture-medium perspective. Trends Biotechnol. 1998;16:323–8.
48. Manning MC, Chou DK, Murphy BM, Payne RW, Katayama DS. Stability of protein pharmaceuticals: an update. Pharm Res. 2010;27:544–75.
49. Gandhi S, Ren D, Xiao G, Bondarenko P, Sloey C, Ricci MS, Krishnan S. Elucidation of degradants in acidic peak of cation exchange chromatography in an IgG1 monoclonal antibody formed on long-term storage in a liquid formulation. Pharm Res. 2012;29:209–24.
50. Harris RJ, Kabakoff B, Macchi FD, Shen FJ, Kwong M, Andya JD, Shire SJ, Bjork N, Totpal K, Chen AB. Identification of multiple sources of charge heterogeneity in a recombinant antibody. J Chromatogr B Biomed Sci Appl. 2001;752:233–45.
51. Patel K, Borchardt RT. Chemical pathways of peptide degradation. II. Kinetics of deamidation of an asparaginyl residue in a model hexapeptide. Pharm Res. 1990;7:703–11.
52. Kaneko Y, Sato R, Aoyagi H. Changes in the quality of antibodies produced by Chinese hamster ovary cells during the death phase of cell culture. J Biosci Bioeng. 2010;109:281–7.
53. Huang L, Lu J, Wroblewski VJ, Beals JM, Riggin RM. *In vivo* deamidation characterization of monoclonal antibody by LC/MS/MS. Anal Chem. 2005;77:1432–9.
54. Liu YD, van Enk JZ, Flynn GC. Human antibody Fc deamidation *in vivo*. Biologicals. 2009;37:313–22.